TOXICOLOGICAL SCIENCES **101(2)**, 350–363 (2008)
doi:10.1093/toxsci/kfm275
Advance Access publication November 5, 2007

o,p′-DDT Elicits PXR/CAR-, Not ER-, Mediated Responses in the Immature Ovariectomized Rat Liver

Naoki Kiyosawa,*,†,‡ Joshua C. Kwekel,*,‡ Lyle D. Burgoon,*,‡ Kurt J. Williams,§ Colleen Tashiro,‖ Brock Chittim,‖ and Timothy R. Zacharewski*,‡,[1]

*Department of Biochemistry and Molecular Biology, Michigan State University, East Lansing, Michigan 48824; †Medicinal Safety Research Laboratories, Daiichi Sankyo Co., Ltd., Shizuoka 437-0065, Japan; ‡Center for Integrative Toxicology, and the National Food Safety and Toxicology Center, Michigan State University, East Lansing, Michigan 48824; §Department of Pathobiology and Diagnostic Investigation, Michigan State University, East Lansing, Michigan 48824; and ‖Wellington Laboratories Inc., Guelph, Ontario N1G 3M5, Canada

Received September 27, 2007; accepted November 1, 2007

Technical-grade dichlorodiphenyltrichloroethane (DDT) is an agricultural pesticide and malarial vector control agent that has been designated a potential human hepatocarcinogen. The *o,p′*-enantiomer exhibits estrogenic activity that has been associated with the carcinogenicity of DDT. The temporal and dose-dependent hepatic estrogenicity of *o,p′*-DDT was investigated using complementary DNA microarrays in immature ovariectomized Sprague-Dawley rats with complementary histopathology and tissue-level analysis. Animals were gavaged with 300 mg/kg *o,p′*-DDT either once or once daily for 3 consecutive days. Liver samples were examined 2, 4, 8, 12, 18, or 24 h after a single dose or following three daily doses. For dose-response studies, a single dose of 3, 10, 30, 100, or 300 mg/kg body weight *o,p′*-DTT was administered for 3 consecutive days. Genes associated with drug metabolism (Cyp2b2 and Cyp3a2), the nuclear receptors constitutive androstane receptor (CAR) and pregnane X receptor (PXR), cell proliferation (Ccnd1, Ccnb1, Ccnb2, and Stmn1), and oxidative stress (Gclm and Hmox1) were significantly induced. Cyp2b2 exhibited dose-dependent regulation and was significantly induced across all time points, while cell proliferation– and oxidative stress–related genes exhibited transient induction. The induction of Cyp2b2 and Cyp3a2 mRNA levels suggest PXR/CAR activation, consistent with expression of genes associated with oxidative stress. Few genes known to be estrogen receptor (ER) regulated were differentially expressed when compared to the hepatic gene expression profile elicited by ethynyl estradiol in immature ovariectomized C57BL/6 mice using the same study design and analysis methods. These data indicate that *o,p′*-DDT elicits PXR/CAR-, not ER-, mediated gene expression in the rat liver. Based on the species-specific differences in CAR regulation, the extrapolation of rodent DDT hepatocarcinogenicity to humans warrants further investigation.

Key Words: **DDT; liver; microarray; CAR; carcinogenesis; estrogen.**

Technical-grade dichlorodiphenyltrichloroethane (DDT) is a mixture of enantiomers and related compounds. DDT and its major metabolites, including 1,1-dichloro-2,2-bis(*p*-chlorophenyl) ethylene and 1,1-dichloro-2,2-bis(*p,p*-chlorophenylethane; DDD), are lipophilic, persistent, and known to bioaccumulate (Bayen *et al*., 2005; Mansour, 2004; Minh *et al*., 2002). The use of DDT was banned in the United States in 1972 due to potential adverse effects in wildlife and humans associated with its estrogenicity and carcinogenicity (Longnecker, 2005; Turusov *et al*., 2002). Nevertheless, it is still used in many countries, especially for malaria vector control due to its overall cost-effectiveness (Attaran and Maharaj, 2000; Weissmann, 2006).

DDT is reported to be a hepatic tumor promoter (Ito *et al*., 1983), with inconclusive genotoxicity activity and a non-genotoxic carcinogen in mice and rats. Although considered to be a risk factor (McGlynn *et al*., 2006), there is no significant correlation between DDT exposure and liver cancer incidence in humans (Cocco *et al*., 2005). Consequently, the International Agency for Research on Cancer (IARC) classifies it as a "possibly carcinogenic (Group 2B)," based on inadequate evidence of carcinogenicity in humans (IARC, 1991).

In the fruit fly, DDT induced glutathione *s*-transferase and xenobiotic-metabolizing enzyme genes mediated by the nuclear receptor DHR90, an ortholog of the rodent constitutive androstane receptor (CAR) and pregnane X receptor (PXR) (King-Jones *et al*., 2006; Pedra *et al*., 2004; Willoughby *et al*., 2006). *Cyp2b* and *Cyp3a* mRNA levels are induced by *p,p′*-DDT, mediated by PXR/CAR (Wyde *et al*., 2003). CAR plays a significant role in tumor carcinogenesis in mice through the induction of drug-metabolizing enzymes and cell proliferation–related genes (Columbano *et al*., 2005; Huang *et al*., 2005; Yamamoto *et al*., 2004). The tumor promotion activity of phenobarbital (PB) is also abolished in *CAR* null mice (Yamamoto *et al*., 2004). Consequently, DDT may act as a PB-type hepatic tumor promoter through CAR activation in rats and mice.

[1] To whom correspondence should be addressed at Department of Biochemistry and Molecular Biology, Michigan State University, East Lansing, MI 48824. Fax: (517) 353-9334. E-mail: tzachare@msu.edu.

In addition to the PB-type enzyme-inducing properties of *p,p′*-DDT in the rodent liver, the *o,p′*-enantiomer exhibits estrogenic activities (Hoekstra *et al*., 2001). Estrogens have also been associated with hepatic tumorigenesis in rodents and humans (Giannitrapani *et al*., 2006), suggesting that the hepatocarcinogenicity of DDT may involve the estrogenic activity of *o,p′*–DDT. Several structurally diverse estrogenic compounds including steroids, industrial chemicals, natural products, and environmental pollutants elicit estrogenic responses in the liver (Ciana *et al*., 2003). Microarray studies have demonstrated that ethynyl estradiol (EE) induces estrogen receptor (ER)–mediated gene expression changes in rodent livers (Boverhof *et al*., 2004; Kato *et al*., 2004). Therefore, the temporal and dose-dependent gene expression activity of *o,p′*-DDT with complementary histopathology and tissue-level analyses were examined to further investigate the PXR-, CAR-, and ER-mediated hepatic activities of *o,p′*-DDT. Collectively, the data indicate that *o,p′*-DDT–elicited hepatic gene expression is not mediated by the ER but rather through PXR/CAR-dependent mechanisms.

MATERIALS AND METHODS

Husbandry. Female Sprague-Dawley rats, ovariectomized on postnatal day 20 were obtained from Charles River Laboratories (Raleigh, NC) on day 25. Rats were housed in polycarbonate cages containing cellulose fiber chip bedding (Aspen Chip Laboratory Bedding, Northeastern Products, Warrensberg, NY) and maintained at 40–60% humidity and 23°C in a room with a 12-h dark/light cycle (7:00 A.M.–7:00 P.M.). Animals were allowed free access to deionized water and Harlan Teklad 22/5 Rodent Diet 8640 (Madison, WI) and acclimatized for 4 days prior to dosing.

Treatments and necropsy. In the dose-response study, rats were orally gavaged once daily for 3 days with 0.1 ml of sesame oil vehicle (Sigma-Aldrich, St Louis, MO) or 3, 10, 30, 100, or 300 mg/kg body weight *o,p′*-DDT (99.2% purity; Sigma-Aldrich) in 0.1 ml of sesame oil vehicle and were sacrificed 24 h after the last treatment. In the time-course study, rats were orally gavaged once or once daily for 3 days with 300 mg/kg body weight *o p′*-DDT in 0.1 ml of sesame oil vehicle. An equal number of time-matched vehicle (VEH) control animals were also dosed in the same manner. Rats receiving one dose were sacrificed 2, 4, 8, 12, 18, and 24 h after treatment. Rats receiving three daily doses were sacrificed 24 h after the third treatment. Treated and vehicle groups consisted of five animals each per time point. The *o,p′*-DDT dose was calculated from average weights of animals prior to treatment. All procedures were performed with the approval of the Michigan State University All-University Committee on Animal Use and Care.

Animals were sacrificed by cervical dislocation, and animal body weights were recorded. Whole liver weights were recorded, and sections of the left lateral lobe (approximately 0.1 g) were snap frozen in liquid nitrogen and stored at − 80°C. The right lateral lobe was placed in 10% neutral-buffered formalin (NBF; VWR International, West Chester, PA) for histopathology and stored at room temperature for at least 24 h prior to further processing.

Histopathology. Following fixation of the right lateral lobe for at least 24 h in 10% NBF, the samples were embedded in paraffin according to standard techniques. Five-micrometer sections were mounted on glass slides and stained with hematoxylin and eosin. All embedding, mounting, and staining of tissues were performed at the Histology/Immunohistochemistry Laboratory (Michigan State University). The histopathology of each liver section was scored according to the National Toxicology Program Pathology guidelines.

Measurement of hepatic o,p′-DDT and o,p′-DDD levels. In the time-course study, one sample from a randomly selected control animal and three randomly selected liver samples from *o,p′*-DDT–treated rats from each time point were processed in parallel with laboratory blanks and a reference or background sample at Wellington Laboratories Inc. (Guelph, Ontario, Canada). Samples were weighed, spiked with $^{13}C^{12}$ *o,p′*-DDT or $^{13}C^{12}$ *o,p′*-DDD surrogate, digested with sulfuric acid, and extracted. Extracts were cleaned, concentrated, and spiked with an injection standard. Analysis was performed on a high-resolution gas chromatograph/high-resolution mass spectrometer (HRMS) using a Hewlett Packard 5890 Series II GC interfaced to a VG 70SE HRMS. The HRMS was operated in the EI/SIR mode at 10,000 resolutions. A 60-m DB5 column (J&W Scientific, Folsom, CA) with an internal diameter of 0.25 mm and film thickness of 0.25 μm was employed. Injection volumes were 2 μl, and a splitless injection was used.

RNA isolation. Total RNA was isolated from left lateral liver sections using Trizol Reagent (Invitrogen, Carlsbad, CA). Samples were removed from − 80°C storage and immediately homogenized in 1 ml Trizol Reagent using a Mixer Mill 300 tissue homogenizer (Retsch, Germany). Total RNA was isolated according to the manufacturer's protocol and resuspended in The RNA Storage Solution (Ambion, Austin, TX). RNA concentrations were determined by spectrophotometry (A_{260}), and purity was assessed by the A_{260}:A_{280} ratio and by visual inspection of 3 μg on a denaturing gel.

Microarray platform. Spotted complementary DNA (cDNA) microarrays were produced in-house from LION Bioscience's Rat cDNA library (LION Bioscience, Heidelberg, Germany). A total of 8565 cDNA features representing 5096 unique genes (confirmed unique Entrez Gene IDs) were selected based on their level of annotation as well as sequence similarity to well-annotated human and mouse genes. Detailed protocols for microarray construction, cDNA probe labeling, sample hybridization, and slide washing can be found at http://dbzach.fst.msu.edu/interfaces/microarray.html. Briefly, PCR-amplified DNA was robotically arrayed onto epoxy-coated glass slides (Schott/Nexterion, Jena, Germany), using an Omnigrid arrayer (GeneMachines, San Carlos, CA) equipped with 32 (8 × 4) Chipmaker 2 pins (Telechem, Sunnyvale, CA) at the Research Technology Support Facility at Michigan State University (http://www.genomics.msu.edu).

Microarray analysis. Dose-response gene expression changes were analyzed using a spoke design in which samples from *o,p′*-DDT–treated animals were cohybridized with VEH animals. Temporal changes in gene expression were assessed using an independent reference design in which samples from *o,p′*-DDT–treated animals were cohybridized with VEH animals. Comparisons were performed between treated and VEH samples using three biological replicates and two independent labelings of each sample (i.e., dye swap) for each time point. Total RNA (25 μg) was reverse transcribed in the presence of Cy3- or Cy5-labeled dUTP (Amersham, Piscataway, NJ) to create fluor-labeled cDNA, which was purified using QIAquick PCR purification kit (Qiagen, Valencia, CA). Cy3- and Cy5-labeled samples were mixed, vacuum dried, and resuspended in 32 μl of hybridization buffer (40% formamide, 4× sodium chloride-sodium citrate, and 1% sodium dodecyl sulfate) with 20 μg polydA and 20 μg of mouse COT-1 DNA (Invitrogen) as a competitor. This probe mixture was heated at 95°C for 2 min and was then hybridized to the array under a 22- × 40-mm Lifterslip (Erie Scientific, Portsmouth, NH) in a light-protected and humidified hybridization chamber (Corning Inc., Lowell, MA). Samples were hybridized for 18–24 h at 42°C in a water bath. Slides were then washed, dried by centrifugation, and scanned at 635 nm (Cy5) and 532 nm (Cy3) on a GenePix 4000B microarray scanner (Molecular Devices, Union City, CA). Images were analyzed for feature and background intensities using GenePix Pro 6.0 (Molecular Devices). All data were managed in the toxicogenomic information management system dbZach relational database (Burgoon *et al*., 2006; Burgoon and Zacharewski, 2007). Microarray data quality was monitored using the laboratory's quality assurance and control plan (Burgoon *et al*., 2005).

Microarray data normalization and statistical analysis. Data were normalized using a semiparametric approach (Eckel *et al*., 2005). Model-based *t*-values were calculated from normalized data, comparing treated and

TABLE 1
QRT-PCR Primer Sequences

Gene name	Gene symbol	Entrez Gene ID	Forward (5′→3′)	Reverse (5′→3′)	Amplicon size
Carbonic anhydrase 3	*Ca3*	54232	TGAGGGCCTCCTTCAAGTAA	ACTGCGGTTTCATCTGACTG	154
Cyclin B1	*Ccnb1*	25203	TTCCGTGTGGGACAGGTAGT	TGGACTACGACATGGTGCAT	125
Cyclin B2	*Ccnb2*	363088	TGAGAAGCACACGATGGAAG	GAACAAATATGCCAGCAGCA	136
Cyclin D1	*Ccnd1*	58919	CACAGTCTGCCCTGTGACAT	GCTGGTCACATGTCTGTGCT	115
Cytochrome P450, family 17, subfamily a, polypeptide 1	*Cyp17a1*	25146	GGCGGGCATAGAGACAACTA	TCGGCTGAAGCCTACGTACT	118
Cytochrome P450, family 2, subfamily b, polypeptide 2	*Cyp2b2*	361523	GGAATGGCCTCATGTTTCTG	TCTTCAGTGCCATTCACAGG	130
Cytochrome P450, family 3, subfamily a, polypeptide 23/polypeptide 1	*Cyp3a23/3a1*	25642	CCTTCCAGCCTTGTAAGGAA	GCAGAACTCCTTGAGGGAAA	143
Cytochrome P450, family 3, subfamily a, polypeptide 11	*Cyp3a2*	266682	GCAAGGTCTGTGATGGAACA	CAAAGGACGAGGACATGGTT	127
Glutamate cysteine ligase, modifier subunit	*Gclm*	29739	CGAGTACCTCAGCAGCCACA	TGTGTGATGCCACCAGATTT	174
Glyceraldehyde-3-phosphate dehydrogenase	*Gapdh*	24383	GTGGACCTCATGGCCTACAT	TGTGAGGGAGATGCTCAGTG	148
Heme oxygenase (decycling) 1	*Hmox1*	24451	GCCTCTACCGACCACAGTTC	GAAAGCTTTTGGGGTTCCTC	170
Nuclear receptor subfamily 1, group I, member 2	*Nr1i2 (PXR)*	84385	TCCACTGCATGCTGAAGAAG	AACCTGTGTGCAGGATAGGG	187
Nuclear receptor subfamily 1, group I, member 3	*Nr1i3 (CAR)*	65035	GGAGGACCAGATCTCCCTTC	GACCGCATCTTCCATCTTGT	130
Proteasome 26S subunit, non-ATPase, 12	*Psmd12*	287772	GGGTTTCGATGACTTCCTGA	GGGGACTCTTAGGCAAGGAC	160
Stathmin 1	*Stmn1*	29332	TTAGTCAGCCTCGGTCTCGT	AGCAAAATGGCAGAGGAGAA	171
Sterol regulatory element–binding factor 1	*Srebf1*	78968	GGGTGAGAGCCTTGAGACAG	GTGGTCTTCCAGAGGCTGAG	178

vehicle responses per time point. Empirical Bayes analysis was used to calculate posterior probabilities ($p1[t]$ value) of activity on a per gene and time point basis using the model-based *t*-value (Eckel *et al*., 2004). Genes were filtered for activity based on the $p1(t)$ value. $p1(t)$ values approaching 1 indicate changes in gene expression that are more robust. In the dose-response study, unique genes with a $p1(t) > 0.999$ and absolute fold change $\geq$ 1.5-fold compared to VEH at least at one time point were initially selected for further investigation. In the time-course study, unique genes with a $p1(t) > 0.999$ in a minimum of two time points and absolute fold change $\geq$ 1.5-fold compared to VEH at least at one time point were selected for further investigation. Functional annotation for differentially expressed genes was obtained using DAVID software (http://david.abcc.ncifcrf.gov/) (Dennis *et al*., 2003). Gene ontology (GO) molecular function was examined for active genes at each time point. Level 2 GO terms with $p < 0.05$ were considered significant. Hierarchical clustering analysis was performed by GeneSpring GX 7.3.1 (Agilent Technologies Inc., Santa Clara, CA).

Quantitative real-time PCR. For each sample, 1.0 μg of total RNA was reverse transcribed by SuperScript II using an anchored oligo-dT primer as described by the manufacturer (Invitrogen). The resultant cDNA (1.0 μl) was used as the template in a 30 μl PCR reaction containing 0.1μM each of forward and reverse gene-specific primers designed using Primer3 (Rozen and Skaletsky, 2000), 3mM $MgCl_2$, 1.0mM deoxynucleoside triphosphates, 0.025 IU AmpliTaq Gold, and 1× SYBR Green PCR buffer (Applied Biosystems, Foster City, CA). Gene names, accession numbers, forward and reverse primer sequences, and amplicon sizes are listed in Table 1. PCR amplification was conducted in MicroAmp Optical 96-well reaction plates (Applied Biosystems) on an Applied Biosystems PRISM 7000 Sequence Detection System using the following conditions: initial denaturation and enzyme activation for 10 min at 95°C, followed by 40 cycles of 95°C for 15 s and 60°C for 1 min. A dissociation protocol was performed to assess the specificity of the primers and the uniformity of the PCR-generated products. Each plate contained duplicate standards of purified PCR products of known template concentration covering six orders of magnitude to interpolate relative template concentrations of the samples from the standard curves of log copy number versus threshold cycle.

TABLE 2
Body Weight and RLW in the Time-Course Study

	Body weight (g)		RLW (%)	
Time (h)	Vehicle	*o*,*p*′-DDT	Vehicle	*o*,*p*′-DDT
2	74.3 ± 2.7	73.5 ± 3.0	4.80 ± 0.10	4.99 ± 0.13
4	75.4 ± 2.8	70.6 ± 4.9	4.75 ± 0.17	4.74 ± 0.07
8	69.3 ± 2.4	78.0 ± 6.4	4.38 ± 0.08	4.81 ± 0.14
12	75.3 ± 3.0	75.3 ± 3.3	4.45 ± 0.15	4.72 ± 0.07
18	80.5 ± 2.2	83.2 ± 2.4	4.38 ± 0.12	4.86 ± 0.15
24	82.4 ± 4.2	78.6 ± 5.0	4.45 ± 0.22	4.98 ± 0.07
72	90.7 ± 2.7	92.9 ± 3.1	5.11 ± 0.13	6.47 ± 0.20*

Note. The data are presented as mean ± SE. The asterisk (*) indicates that the RLW was significantly higher ($p < 0.05$) in 300 mg/kg *o*,*p*′-DDT–treated rats at 72 h when compared to time-matched vehicle control in the time-course study in the absence of any effect on body weight using a two-way ANOVA followed by Tukey's post hoc test.

TABLE 3
Liver Histopathology Following *o,p′*-DDT Treatment in Time-Course Study

	Time (h)						
Histological findings	2	4	8	12	18	24	72
Swelling							
Centrilobular	Mild (2/5)	Mild (4/5)	—	—	—	—	—
Centrilobular-midzonal	Moderate (2/5), moderate to marked (1/5)	Moderate (1/5)	Mild (1/5), moderate (4/5)	Mild (2/5) Mild-moderate (2/5) Moderate (1/5)	Mild (2/5)	—	—
Eosinophila							
Centrilobular	Mild (2/5)	—	—	—	—	—	—
Centrilobular-midzonal	Moderate (2/5)	Moderate (1/5)	—	Mild (2/5) Mild-moderate (2/5) Moderate (1/5)	—	—	—

Note. The numbers in parentheses indicate the number of animals in the *o,p′*-DDT–treated group exhibiting the pathology.

The copy number of each unknown sample for each gene was standardized to that of glyceraldehyde-3-phosphate dehydrogenase gene to control for differences in RNA loading, quality, and cDNA synthesis. Microarray data for *Ccnd3* gene (Entrez Gene ID: 25193) was not concordant with the quantitative real-time PCR (QRT-PCR) results and therefore excluded from further analysis.

Correlation analysis between o,p′-DDT–treated rat and EE-treated mouse livers. Genes with a $p1(t) > 0.99$ and absolute fold change $\geq$ 1.5-fold at one or more time points in the *o,p′*-DDT–treated rat liver samples were selected and used for correlation analysis (Burgoon *et al*., 2006), against our previously published EE-treated mouse liver gene expression data (see http://www.bch.msu.edu/~zacharet/publications/supplementary/index.html for EE data). Orthologous rat and mouse genes were identified using Homologene (http://www.ncbi.nlm.nih.gov/sites/entrez?db=homologene). The filtering criteria used for the correlation analysis were relaxed compared to that used in the GO analysis to include more ortholog comparisons in the correlation analysis and thus be more informative of the overall similarity between the two data sets. The correlation analysis involved a multivariate correlation–based visualization application that was developed in-house (Burgoon *et al*., 2006) and has been previously used to investigate the estrogenicity of 2,3,7,8-tetrachlrodibenzo-*p*-dioxin in the mouse uterus when compared to EE (Boverhof *et al*., 2006). This tool calculates the temporal correlations between gene expression and significance values for orthologous DDT-treated rat (this study) and EE-treated mouse genes (Boverhof *et al*., 2004) and summarizes the results in a scatterplot.

Statistical analysis. Body weight, relative liver weight (RLW), and QRT-PCR data are presented as the mean ± SE. Statistical analysis was performed with two-way ANOVA followed by Tukey's post hoc test between VEH and *o,p′*-DDT–treated groups ($p < 0.05$). Hepatic *o,p′*-DDT and *o,p′*-DDD concentration data were analyzed using a two-way ANOVA to identify significant differences in *o,p′*-DDT and *o,p′*-DDD concentrations across time. Pairwise comparisons were performed using Tukey's honestly significant difference post hoc test to control type I error ($\alpha = 0.05$). For QRT-PCR data, the relative expression levels of target genes were scaled such that the standardized expression level of the time-matched VEH group was equal to 1 for graphing purposes. All statistics were performed using SAS 9.1.3 software (SAS Institute Inc., Cary, NC).

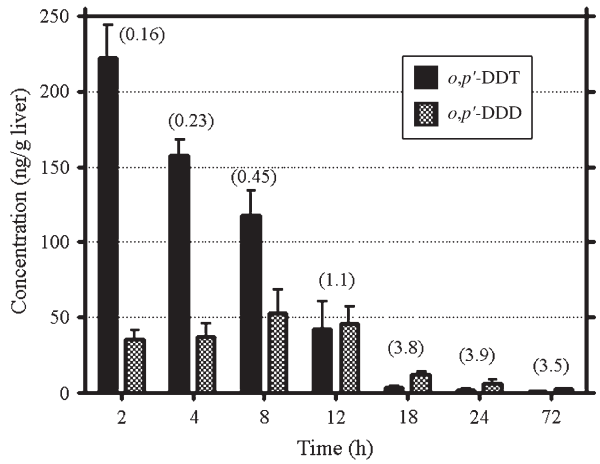

FIG. 1. Hepatic *o,p′*-DDT and *o,p′*-DDD levels in time-course study. Hepatic *o,p′*-DDT and *o,p′*-DDD levels were determined using high-resolution gas chromatograph/HRMS from three randomly selected rats orally gavaged with 300 mg/kg *o,p′*-DDT. Numbers in parentheses show the *o,p′*-DDD/*o,p′*-DDT concentration ratio. The data are presented as mean ± SE.

RESULTS

Body Weight, RLW, and Histopathology

There was no significant difference between VEH and *o,p′*-DDT–treated animal body and RLWs in the dose-response study at 72 h (data not shown). RLWs were significantly higher in 300 μg/kg *o,p′*-DDT–treated rats at 72 h when compared to VEH in the time-course study in the absence of any effect on body weight (Table 2), consistent with the increase in RLW in rats treated with 106 mg/kg *p,p′*-DDT (Tomiyama *et al*., 2003). Thus, 300 μg/kg *o,p′*-DDT was used in the time-course study.

There were also no significant signs of irreversible hepatocellular injury at any time point. Hepatocytes exhibited early centrilobular and midzonal swelling with hypertrophy and eosinophilic staining (Table 3). However, there was no evidence of hepatocyte swelling with hypertrophy and eosinophilia after 18 h, and therefore, the 72 h dose-response sections were not examined.

	Number of active genes	Time (h) 2	4	8	12	18	24	72	Representative genes
	Up-regulated	12	13	21	42	225	81	31	
	Down-regulated	6	18	24	26	38	6	24	
GO term / Number of genes classified	Oxidoreductase activity	4	4	9	12	20	10	8	*Cyp2b2, Cyp3a2, Por, Gpx2, Akr7a2, Aldh1a1, etc.*
	Electron transporter activity	2	3	5	5	8	6	4	*Txn1, Txnrd1, Por, Aldh1a1, Me1, Akr7a2, etc.*
	Tetrapyrrole binding	1	2	4	5	7	2	4	*Cyp2b2, Cyp3a2, Cyp17a1, App, etc.*
	Structural constituent of ribosome	1	1	1	1	15	3	3	*Rps3, Rps6, Rpl6, Rpl13, etc.*
	Protein binding	2	4	11	18	80	28	15	*Ccnd1, Stmn1, Hspd1, Psmb1, Psmc3, Prkcdbp, App, etc.*
	Transcription cofactor activity	0	0	1	1	11	3	0	*Psmc3, Psmc5, Hes6, Taf9, etc.*
	Ligase activity	0	3	2	4	12	0	2	*Gclm, Eprs, Mdm2_predicted, Lig1, Asns, Lars, etc.*
	Proteasome endopeptidase activity	0	0	0	0	6	4	0	*Psma4, Psma5, Psma6, Psmb1, Psmb4, Psmb5*
	Nucleotide binding	0	0	1	7	36	15	6	*Tuba1, Ran, Tk1, Hspca, Hspcb, Hspe1, Arf4, Tuba1, etc.*
	Nitric-oxide synthase regulator activity	0	0	0	1	2	2	0	*Hspca, Calm1*
	Thioredoxin-disulfide reductase activity	0	0	0	1	2	2	0	*Txn1, Txnrd1*
	Hydrolase activity	2	2	5	10	34	15	5	*Ces6, Ephx1, Psma4, Psma5, Tubb5, Rab14, Usp14, etc.*
	Pattern binding	0	0	0	0	5	2	3	*Apoh, Fgfr2, App*

$p<0.05$ $p<0.01$

FIG. 2. Functional annotation of differentially expressed genes following *o,p′*-DDT treatment in the time-course study. Differentially expressed genes were selected based on a $p1(t) > 0.999$ at two or more time points and an absolute fold change ≥ 1.5 at one or more time points relative to time-matched vehicle controls. Functional annotation of selected genes was obtained from the GO database using DAVID (http://david.abcc.ncifcrf.gov). GO functions were examined for active genes at each time point, and level 2 GO terms with $p < 0.05$ were considered significant. The number in each cell indicates the number of active genes that were classified in the GO term. Gray and black shading indicate $p < 0.05$ and $p < 0.01$, respectively. Representative genes associated with the GO terms are shown to the right. Note that not all genes are annotated with a GO functional term and that a gene can be associated with more than one function.

Hepatic o,p′-DDT and o,p′-DDD Concentrations in Time-Course Study

The time-dependent accumulation and elimination of hepatic *o,p′*-DDT has not been previously reported using a comparable study design. Following an initial accumulation, *o,p′*-DDT and *o,p′*-DDD levels decreased over time. *o,p′*-DDT concentrations were only significantly different from *o,p′*-DDD at 2 h. The levels of *o,p′*-DDT were highest at 2 h (222 ng/g liver), which dramatically decreased in a time-dependent manner to 0.68 ng/g liver at 72 h (Fig. 1). In contrast, the levels of *o,p′*-DDD modestly increased to 35.1–52.7 ng/g liver at 12 h and then decreased to 5.8 ng/g liver by 24 h. *o,p′*-DDT concentrations continued to decrease (2.4 ng/g liver at 72 h),

TABLE 4
Differentially Expressed Drug Metabolism, Sterol Metabolism, and Cell Proliferation–Related Genes Following *o,p′*-DDT Treatment

Gene name	Gene symbol	Entrez Gene ID	Time (h)[a] 2	4	8	12	18	24	72
Drug metabolism									
Aldehyde dehydrogenase family 1, member A1	*Aldh1a1*	24188	0.96	0.94	**1.79**	**2.33**	**2.35**	**2.97**	**3.17**
Cytochrome P450, family 2, subfamily b, polypeptide 2	*Cyp2b2*	361523	**2.24**	**5.67**	**6.12**	**4.98**	**4.99**	**5.68**	**5.73**
Cytochrome P450, family 2, subfamily c, polypeptide 23	*Cyp2c23*	83790	1.09	0.84	0.80	**0.70**	**0.50**	**0.71**	0.89
Cytochrome P450, family 3, subfamily a, polypeptide 11	*Cyp3a2*	266682	1.05	1.16	**2.02**	**1.76**	**2.02**	**1.71**	**2.35**
Glutathione *s*-transferase theta 1	*Gstt1*	25260	0.91	0.84	0.80	**0.75**	**0.65**	0.90	1.04
Glutathione *s*-transferase A3	*Gsta3*	24421	0.99	0.90	0.88	1.17	1.24	**1.47**	**1.63**
P450 (cytochrome) oxidoreductase	*Por*	29441	1.67	**1.89**	**2.00**	**2.05**	**2.65**	**1.80**	**1.82**
Sterol metabolism									
7-Dehydrocholesterol reductase	*Dhcr7*	64191	0.90	0.77	**0.62**	**0.69**	0.84	1.15	1.09
Cytochrome P450, family 17, subfamily a, polypeptide 1	*Cyp17a1*	25146	0.87	1.08	1.09	**0.55**	**0.58**	0.85	**0.61**
Oxysterol-binding protein–like 1A	*Osbpl1a*	259221	0.98	0.88	**0.82**	0.92	0.93	**0.85**	**0.65**
SREBP cleavage activating protein (predicted)	*Scap_predicted*	301024	1.00	0.80	0.74	**0.68**	**0.64**	**0.67**	0.79
Sterol regulatory element–binding factor 1	*Srebf1*	78968	0.82	**0.55**	**0.33**	**0.59**	0.63	0.77	0.93
Cell proliferation									
Cyclin B2	*Ccnb2*	363088	0.89	1.10	0.84	0.77	1.02	**1.67**	**0.69**
Cyclin D1	*Ccnd1*	58919	0.94	1.11	1.24	**2.03**	**2.01**	0.72	**0.53**
Stathmin 1	*Stmn1*	29332	1.03	1.16	0.88	0.99	**1.61**	**1.77**	**0.69**
Transformed mouse 3T3 cell double minute 2 homolog (mouse) (predicted)	*Mdm2_predicted*	314856	1.09	1.22	**1.42**	**2.06**	**2.51**	1.29	1.03

[a]Values in bold indicate expression ratio where $p1(t) > 0.999$.

TABLE 5
Differentially Expressed Electron Transport, Reductive Reaction, and Stress Response–Related Genes Following *o,p′*-DDT Treatment

Gene name	Gene symbol	Entrez Gene ID	Time (h)[a] 2	4	8	12	18	24	72
Electron transport/reductive reactions									
Aldo-keto reductase family 7, member A2	*Akr7a2*	171445	**2.61**	1.57	**3.11**	**2.60**	**3.53**	1.18	1.55
Epoxide hydrolase 1, microsomal	*Ephx1*	25315	1.16	1.02	1.35	**1.90**	**2.67**	**2.40**	**2.48**
Ferritin light chain 1	*Ftl1*	29292	1.09	0.89	0.87	0.92	1.25	**1.55**	**1.28**
Glutamate cysteine ligase, modifier subunit	*Gclm*	29739	0.91	**0.64**	0.78	1.08	**2.07**	1.50	1.22
Glutamate-cysteine ligase, catalytic subunit	*Gclc*	25283	1.01	0.63	0.68	1.23	**1.50**	1.39	1.03
Glutathione peroxidase 2	*Gpx2*	29326	0.86	0.86	0.95	1.13	**2.25**	**1.72**	**1.58**
Thioredoxin 1	*Txn1*	116484	0.96	1.00	1.00	1.11	**1.67**	**1.70**	**1.37**
Thioredoxin reductase 1	*Txnrd1*	58819	0.91	0.86	0.95	**1.87**	**2.45**	**1.59**	0.92
Stress responsive									
Heat shock 10 kDa protein 1 (chaperonin 10)	*Hspe1*	25462	1.06	1.01	1.02	**1.38**	**1.61**	**1.43**	1.12
Heat shock 90 kDa protein 1, beta	*Hspcb*	301252	0.93	0.89	1.00	1.23	**1.51**	**1.39**	1.14
Hsp 1 (chaperonin)	*Hspd1*	63868	1.03	1.04	1.11	**1.32**	**1.67**	**1.45**	**1.21**
Hsp 1, alpha	*Hspca*	299331	0.87	0.89	1.00	**1.90**	**2.78**	**2.29**	1.25
Heat shock 90 kDa protein 1, alpha-like 3 (predicted)	*Hspcal3_predicted*	297852	0.88	0.89	0.97	**1.88**	**2.65**	**2.23**	1.18
Heme oxygenase (decycling) 1	*Hmox1*	24451	0.84	0.93	0.96	**2.47**	**3.13**	1.23	0.95
Similar to DnaJ (Hsp40) homolog, subfamily B, member 10 isoform 2	*LOC689593*	689593	0.97	0.87	1.00	**1.17**	**1.54**	1.02	0.88
DnaJ (Hsp40) homolog, subfamily C, member 2	*Dnajc2*	116456	0.88	0.99	0.97	**1.24**	**1.53**	1.02	0.83
Poly (ADP-ribose) polymerase family, member 1	*Parp1*	25591	1.12	1.04	**1.53**	**1.43**	**1.80**	**1.40**	1.13
Poly (ADP-ribose) polymerase family, member 2 (predicted)	*Parp2_predicted*	290027	1.03	0.95	1.08	**1.21**	**1.83**	**1.56**	1.09
Miscellaneous									
Amyloid beta (A4) precursor protein	*App*	54226	0.96	0.98	1.03	**1.22**	**1.61**	**1.23**	1.10
Carbonic anhydrase 3	*Ca3*	54232	0.66	0.83	0.73	0.59	**0.23**	**0.30**	0.91
Carboxylesterase 6	*Ces6*	246252	1.11	1.50	1.11	1.24	**1.88**	**1.99**	**2.28**
Double C2, gamma	*Doc2g*	293654	**1.66**	**3.32**	**5.27**	**4.93**	**5.63**	**5.37**	**3.73**
Insulin-like growth factor 1	*Igf1*	24482	1.02	0.91	0.78	0.85	**0.68**	**0.63**	0.77
Insulin-like growth factor–binding protein 3	*Igfbp3*	24484	0.89	0.99	0.98	0.96	0.92	**0.78**	**0.60**
Interferon regulatory factor 1	*Irf1*	24508	**0.44**	**0.61**	**0.60**	0.82	0.81	1.14	1.06
RAN, member RAS oncogene family	*Ran*	84509	0.99	1.00	0.97	**1.28**	**1.89**	**1.43**	1.05

[a]Values in bold indicate expression ratio where $p1(t) > 0.999$.

suggesting that treatment enhanced its hepatic clearance. The levels of *o,p′*-DDD were higher compared to *o,p′*-DDT after 12 h, and the *o,p′*-DDD/*o,p′*-DDT ratio showed a time-dependent increase from 2 h (ratio: 0.16) to 72 h (ratio: 3.5), suggesting that *o,p′*-DDT was metabolized to *o,p′*-DDD. *o,p′*-DDT and *o,p′*-DDD levels were not examined in the dose-response study samples and were not detected in the liver samples from VEH animals in the time-course study.

Microarray Analysis

All the microarray data for both the dose response and the time-course studies are provided as Supplementary Tables 1 and 2, respectively. In the time-course study, 327 unique genes were differentially expressed following treatment (Fig. 2, Tables 4–6). In addition, there was a clear dose-dependent increase in the number of differentially expressed genes (Fig. 3a). Of the 81 genes induced at 72 h in the time-course study, 58 exhibited dose-dependent induction, although none achieved a plateau, thus precluding Effective dose, 50% (ED_{50}) determinations (Fig. 3). GO analysis indicated that genes associated with oxidoreductase activity such as *Cyp2b2* or *Cyp3a2* were induced as early as 2 h (Table 4), while electron transport genes related to reductive reactions (e.g., *Txn1*, *Txnrd1*, *Por*, *Aldh1a1*, and *Akr7a2*) exhibited differential expression as early as 4 h (Table 5), which persisted to 72 h.

Both the number of active genes and overrepresented GO terms were highest at 18 h. Diverse biological responses such as protein synthesis (GO term: structural constituent of ribosome) and degradation (GO term: proteasome endopeptidase activity) were represented (Table 6). Many eukaryotic translational initiation factors, and proteasome-related and ribosomal protein genes were induced at 18 h. In addition, the stress-responsive heat shock protein (*HSP*) and *Hmox1* genes were induced as well as *Gclm* and *Gpx2* genes, which are involved in glutathione homeostasis, at 18 and 24 h. Genes involved in electron transport or reductive reactions such as *Ephx1*, *Flt1*, and *Txn1* were also induced at 18 h.

TABLE 6
Differentially Expressed Protein Turnover–Related Genes Following *o,p′*-DDT Treatment

Gene name	Gene symbol	Entrez Gene ID	Time (h)[a] 2	4	8	12	18	24	72
Protein synthesis/degradation									
Eukaryotic translation initiation factor 2, subunit 2 (beta)	*Eif2s2*	296302	1.00	1.02	1.10	**1.35**	**1.77**	1.08	0.97
Eukaryotic translation initiation factor 3, subunit 8, 110 kDa	*Eif3s8*	293484	1.04	1.02	1.12	**1.25**	**1.69**	1.07	1.05
Eukaryotic translation initiation factor 4E–binding protein 1	*Eif4ebp1*	116636	1.08	0.95	1.26	**1.32**	**1.68**	1.29	1.08
Similar to mitochondrial ribosomal protein 63	*LOC691814*	691814	0.91	0.98	1.52	**1.87**	**1.96**	1.49	0.96
Mitochondrial ribosomal protein S12 (predicted)	*Mrps12_predicted*	292758	1.05	1.02	1.21	**1.43**	**1.47**	**1.64**	**1.81**
Proteasome (prosome, macropain) 26S subunit, ATPase 3	*Psmc3*	29677	0.99	0.97	1.09	**1.32**	**1.85**	**1.56**	1.21
Proteasome (prosome, macropain) 26S subunit, ATPase, 4	*Psmc4*	117262	0.91	0.90	1.03	**1.25**	**1.82**	**1.47**	1.15
Proteasome (prosome, macropain) 26S subunit, non-ATPase, 1	*Psmd1*	83806	0.97	0.91	0.95	**1.27**	**1.89**	**1.54**	1.14
Proteasome (prosome, macropain) 26S subunit, non-ATPase, 11 (predicted)	*Psmd11_predicted*	303353	0.96	0.91	1.09	**1.41**	**1.99**	**1.54**	1.18
Proteasome (prosome, macropain) 26S subunit, non-ATPase, 12	*Psmd12*	287772	0.98	0.96	1.08	**1.42**	**2.17**	**1.50**	**1.19**
Proteasome (prosome, macropain) 26S subunit, non-ATPase, 2	*Psmd2*	287984	0.96	0.96	1.02	1.18	**1.85**	**1.62**	**1.32**
Proteasome (prosome, macropain) 26S subunit, non-ATPase, 4	*Psmd4*	83499	0.91	0.91	1.01	**1.27**	**1.88**	**1.45**	1.08
Proteasome (prosome, macropain) 26S subunit, non-ATPase, 8	*Psmd8*	292766	0.95	0.99	1.08	**1.25**	**1.91**	**1.74**	**1.40**
Proteasome (prosome, macropain) subunit, alpha type 4	*Psma4*	29671	0.93	0.94	1.00	**1.24**	**1.75**	**1.53**	**1.21**
Proteasome (prosome, macropain) subunit, alpha type 5	*Psma5*	29672	0.94	0.90	1.07	**1.30**	**2.00**	**1.52**	**1.20**
Proteasome (prosome, macropain) subunit, alpha type 6	*Psma6*	29673	0.93	1.04	1.05	**1.24**	**1.68**	**1.40**	**1.21**
Proteasome (prosome, macropain) subunit, beta type 1	*Psmb1*	94198	0.98	0.94	1.04	1.23	**1.58**	**1.47**	1.20
Proteasome (prosome, macropain) subunit, beta type 4	*Psmb4*	58854	0.99	1.00	1.06	**1.17**	**1.73**	**1.56**	**1.27**
Proteasome (prosome, macropain) subunit, beta type 5	*Psmb5*	29425	1.10	0.98	1.09	**1.22**	**1.74**	**1.59**	**1.37**
Similar to ribosomal protein L10a (predicted)	*RGD1560124_predicted*	302497	1.18	1.09	**1.18**	**1.23**	**1.56**	**1.26**	1.10
Ribosomal protein L13	*Rpl13*	81765	1.12	1.07	1.15	**1.20**	**1.56**	**1.31**	1.10
Ribosomal protein L18	*Rpl18*	81766	1.09	1.03	1.09	**1.22**	**1.55**	**1.28**	1.07
Ribosomal protein L23	*Rpl23*	29282	1.09	1.04	1.10	**1.15**	**1.57**	**1.23**	0.98
Ribosomal protein L3	*Rpl3*	300079	1.06	1.06	**1.24**	**1.21**	**1.60**	**1.24**	0.97
Ribosomal protein L37	*Rpl37*	81770	1.05	1.05	1.11	**1.21**	**1.52**	**1.20**	1.06
Ribosomal protein L6	*Rpl6*	117042	1.08	1.03	1.11	1.18	**1.61**	**1.24**	1.03
Ribosomal protein P0–like protein	*RGD1311709_predicted*	298586	1.00	1.03	1.10	**1.42**	**1.80**	1.21	0.93
Ribosomal protein S15a	*Rps15a*	117053	**1.21**	1.07	1.11	**1.22**	**1.71**	**1.31**	1.09
Ribosomal protein S17	*Rps17*	29286	1.07	1.05	1.10	1.12	**1.55**	**1.26**	1.06
Ribosomal protein S20	*Rps20*	122772	1.12	1.14	1.10	**1.17**	**1.62**	**1.33**	1.12
Ribosomal protein S3	*Rps3*	140654	1.06	1.05	1.12	**1.20**	**1.57**	**1.30**	1.10
Ribosomal protein S5	*Rps5*	25538	1.13	1.10	1.14	1.20	**1.55**	**1.36**	1.13
Ribosomal protein S6	*Rps6*	29304	**1.16**	**1.09**	**1.17**	**1.25**	**1.70**	**1.31**	**1.10**
Ribosomal protein S7	*LOC497813*	497813	1.06	1.03	1.15	1.09	**1.56**	**1.28**	1.08
Ribosomal protein S8	*Rps8*	65136	1.09	1.09	1.12	**1.24**	**1.63**	**1.28**	1.09
Ribosomal protein SA	*Rpsa*	29236	1.11	1.12	**1.20**	**1.22**	**1.59**	**1.35**	**1.42**

[a]Values in bold indicate expression ratio where $p1(t) > 0.999$.

Several sterol metabolism– and cell proliferation–related genes were also differentially expressed (Table 4). The sterol metabolism–related gene, Srebf1, was repressed 4–18 h along with another sterol metabolism–related gene, *Cyp17a1*, at 12–18 h. Genes associated with cell proliferation, including *Ccnb1*, *Ccnb2*, *Mdm2_predicted*, and *Stmn1*, exhibited induction by *o,p′*-DDT.

Quantitative Real-Time PCR

In total, 15 genes identified as being differentially regulated by *o,p′*-DDT in the microarray time-course study, including other genes known to be regulated by PXR/CAR that were not represented on our cDNA array, were examined by QRT-PCR. QRT-PCR confirmed that the PXR/CAR-regulated drug-metabolizing genes, *Cyp2b2*, *Cyp3a2*, and *Cyp3a23/3a1*, were induced by *o,p′*-DDT when compared to VEH (Fig. 4). Moreover, the expression of *CAR* (*Nrli3*) and *PXR* (*Nrli2*) mRNA, which regulate *Cyp2b* and *Cyp3a*, respectively, were also induced (Fig. 4). The cell proliferation genes, *Ccnb1*, *Ccnb2*, *Ccnd1*, and *Stmn1*, also exhibited comparable microarray and QRT-PCR expression profiles (Fig. 5). Overall, there was a good correlation between the 12 genes examined by microarray and QRT-PCR (Figs. 4–6).

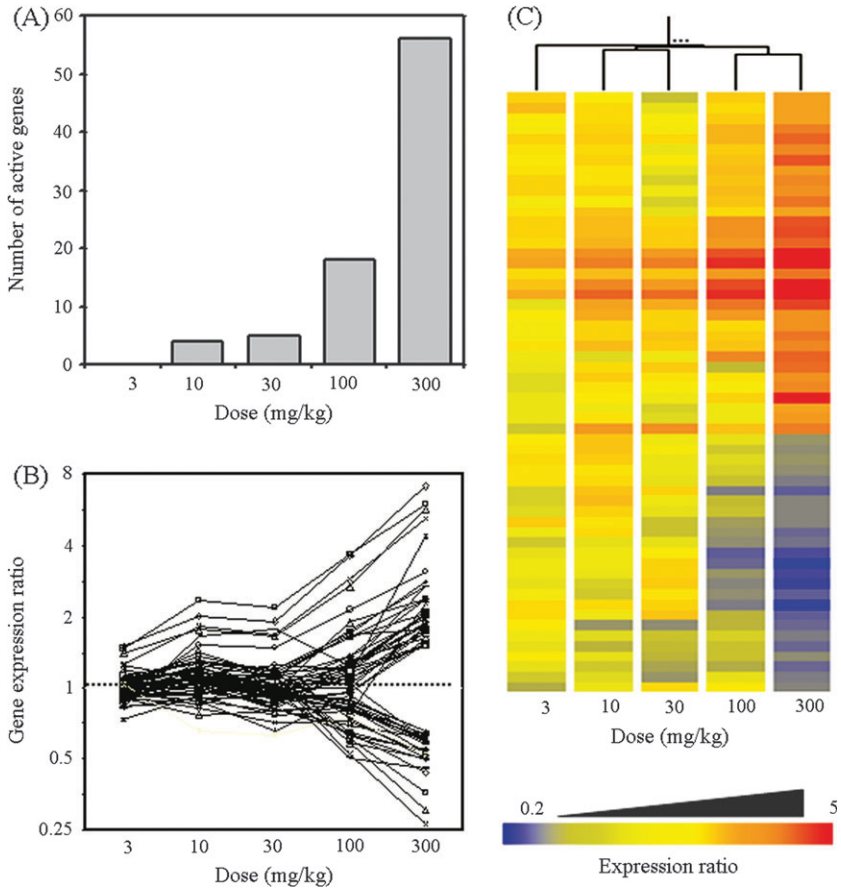

FIG. 3. Summary of microarray analysis in dose-response study. (A) Number of differentially expressed genes. Differentially expressed genes were selected using a $p1(t) > 0.999$ combined with an absolute fold change $\geq$1.5 relative to time-matched vehicle controls. (B) Dose-response profiles of differentially expressed genes and (C) hierarchical clustering of differentially expressed genes. The expression level of each differentially regulated gene relative to time-matched vehicle control is represented as a line graph (B) and a heat map (C), respectively.

Comparison of o,p′-DDT– and EE-Induced Hepatic Gene Expression Profiles

In order to comprehensively compare hepatic *o,p′*-DDT–elicited gene expression with a similar study in EE-treated mice, the filtering criteria for the *o,p′*-DDT rat data were relaxed ($p1[t] > 0.99$, 1.5-fold change) and the resulting genes that had overlapping orthologs in the mouse EE data set were subsequently compared. In total, 148 orthologous gene pairs were identified between the two data sets (Fig. 7A and Supplementary Table 3). In order to ascertain the similarity of expression profiles between *o,p′*-DDT in the rat liver and EE in the mouse liver, a Pearson's correlation analysis was performed on the temporal gene expression (fold change) and significance ($p1[t]$ value for rat and transformed *t*-value for mouse data, respectively) profiles. Note that the *o,p′*-DDT and EE gene expression studies used the same design, model, microarray platform, and data analysis methods. The paired data, representing 148 orthologous rat and mouse genes, are plotted on a coordinate axis with the x-axis providing an index of the gene expression similarity and the y-axis providing an index of the significance similarity for each orthologous pair present in the *o,p′*-DDT and EE data sets. Ideally, well-correlated genes (i.e., exhibiting similar gene expression and significance profiles) aggregate in the upper right quadrant. Figure 7B illustrates that the correlations between the orthologous genes appear randomly distributed throughout the plot, indicating a poor correlation between the *o,p′*-DDT–treated rat liver and EE-treated mouse liver data sets.

More specifically, *Igfbp1*, *Col4a1*, *Myh3*, *Ggt1*, *Stat5a*, and *Cyp17a1* exhibited induction following EE treatment, suggesting ER-mediated regulation of the expression of these genes in the mouse liver. However, the rat orthologs of these genes were not induced by *o,p′*-DDT (Supplementary Table 3). Moreover, the expression of the steroidogenesis-associated gene Cyp17a1 was repressed in the rat liver and verified by QRT-PCR (Fig. 6).

DISCUSSION

The estrogenicity of *o,p*-DDT is well established. A comprehensive time-course and dose-response cDNA microarray

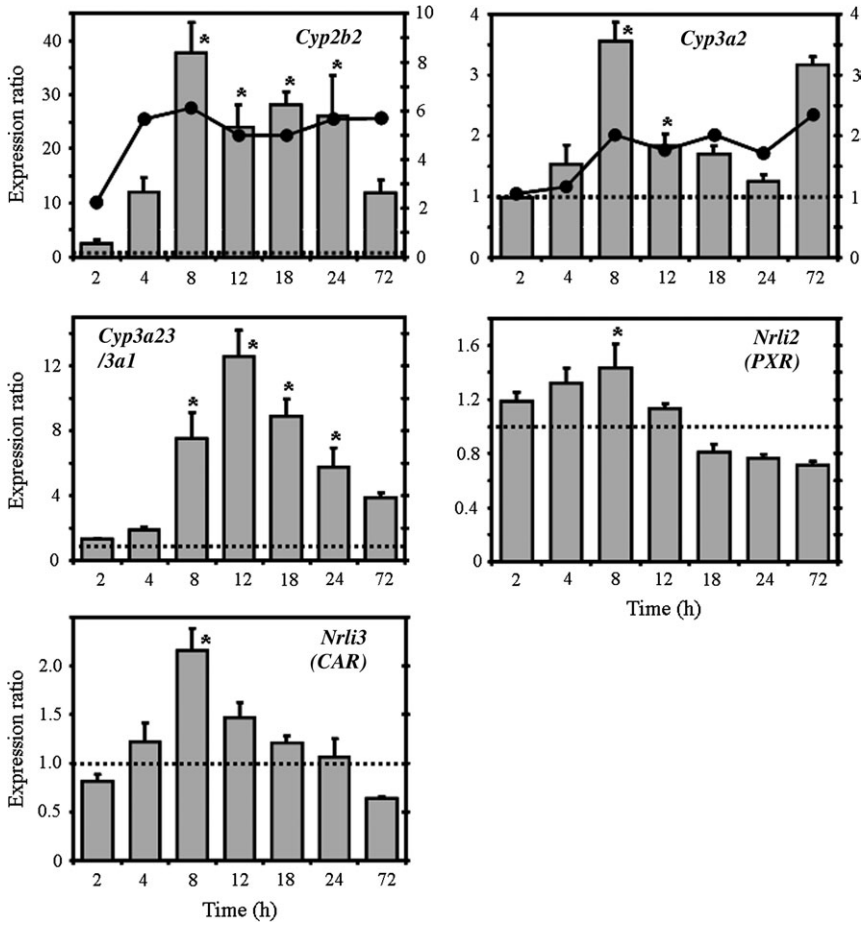

FIG. 4. QRT-PCR and microarray analysis of nuclear receptors and drug metabolism–related genes. CAR (Nrli3) and PXR (Nrli2) regulate Cyp2b and Cyp3a, respectively. QRT-PCR results relative to time-matched vehicle controls are shown as bars (left axis) and presented as mean ± SE. Microarray results are represented as lines (right axis). The dashed line indicates the expression level of the time-matched vehicle control. Features for Cyp3a23/3a1, Nrli2, and Nrli3 were not represented on the cDNA array and were only examined by QRT-PCR. The asterisk (*) indicates a significant ($p < 0.05$) difference from the time-matched vehicle controls using a two-way ANOVA followed by Tukey's post hoc test for QRT-PCR data.

study with complementary histopathology and *o,p′*-DDT tissue-level analysis was completed to further investigate its estrogenicity and potential role in hepatocarcinogenicity.

The gene expression profile of *o,p′*-DDT was characteristic of a PB-type inducer, as opposed to an estrogen. This is consistent with the *p,p′*-DDT induction of PB-type enzyme activity in rat liver (Wyde *et al.*, 2003). *o,p′*-DDT induced *Cyp2b2*, *Cyp3a2*, and *Cyp3a23/3a1* genes, indicative of CAR/PXR regulation (Sparfel *et al.*, 2003). PB is reported to induce *Cyp2b2* transcript levels sevenfold in the rat liver (Agrawal and Shapiro, 2003) and *Cyp2b1/2* mRNA levels fivefold in primary hepatocytes (Ganem *et al.*, 1999). In the present study, *o,p′*-DDT induced *Cyp2b2* mRNA levels approximately 30-fold in the liver. Dexamethazone, a potent PXR activator, induced *Cyp3a2* transcripts fourfold in the male rat liver (Meredith *et al.*, 2003). *Cyp3a23/3a1* was also induced 35-fold by dexamethazone and 10-fold by PB in the male rat liver (Martignoni *et al.*, 2004), whereas it is induced sevenfold by 16α-carbonitrile, a potent PXR activator, in the adult female rat liver (Guzelian *et al.*, 2006). In the present study, *o,p′*-DDT induced the *Cyp3a2* 3.5-fold and *Cyp3a23/3a1* 12-fold in immature ovariectomized C57BL/6 liver. Collectively, the induction levels of *Cyp2b2*, *Cyp3a2*, and *Cyp3a23/3a1* mRNA by *o,p′*-DDT are comparable to other well-established PXR/CAR ligands.

CAR activation is associated with hepatomegaly (Huang *et al.*, 2005) and centrilobular hypertrophy with concomitant induction of *Cyp2b1* and *Cyp3a2*, which is prototypical of PB-type enzyme inducers (Harada *et al.*, 2003). Furthermore, both *CAR* and *PXR* transcript levels were induced, which may facilitate receptor-mediated differential gene expression. However, cDNA microarrays and QRT-PCR only assess transcript levels, while increases in mRNA levels may also be due to posttranscriptional events (e.g., mRNA stability).

The activation of PXR/CAR and the induction of cytochrome P450 activity is not only consistent with the increases

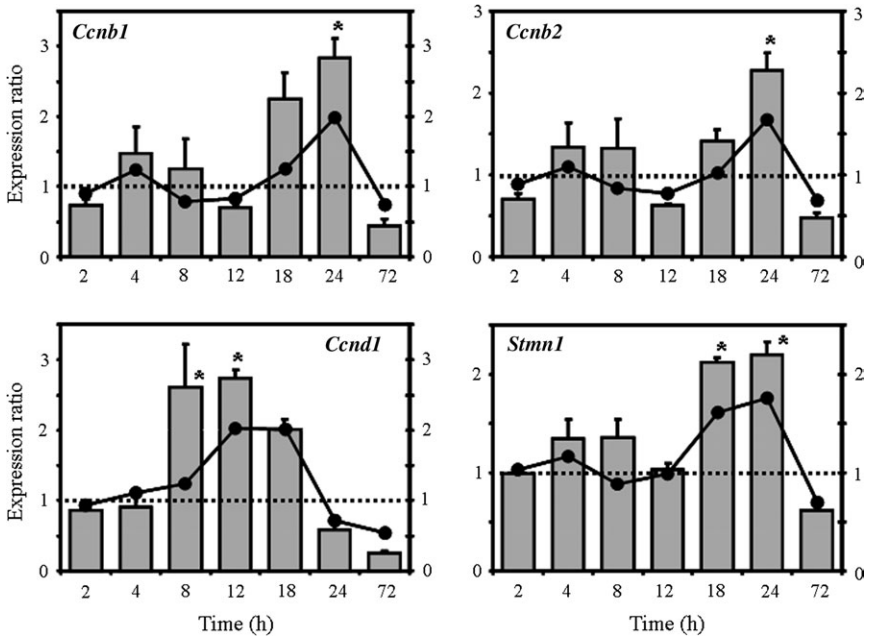

FIG. 5. QRT-PCR and microarray results for representative cell proliferation–related genes. Microarray and QRT-PCR results exhibit good correlations for Ccnb1, Ccnb2, Ccnd1, and Stmn1. The QRT-PCR results relative to time-matched vehicle controls are shown as bars (left axis), and microarray results are represented as lines (right axis). The QRT-PCR data are presented as mean ± SE. The dashed line indicates the expression level of the time-matched vehicle control. The asterisk (*) indicates a significant ($p < 0.05$) difference from the time-matched vehicle controls using a two-way ANOVA followed by Tukey's post hoc test for QRT-PCR data.

in RLW and hepatocyte swelling with hypertrophy but also with the hepatic clearance of *o,p′*-DDT, which bears similarities to the reductive dechlorination of *p,p′*-DDT to *p,p′*-DDD by Cyp2b and Cyp3a isozymes in the rat liver (Kitamura *et al.*, 2002). Therefore, the induction of *Cyp2b2*, *Cyp3a2*, and *Cyp3a23/3a1* mRNA levels likely contributes to the time-dependent clearance of *o,p′*-DDT and the detection of *o,p′*-DDD from 2 to 12 h as well as its subsequent decrease, as seen with metabolism of *p,p′*-DDT (Tebourbi *et al.*, 2006; Tomiyama *et al.*, 2003). Furthermore, *p,p′*-DDT and its metabolites accumulate in adipocytes with relatively low levels present in the liver (Tebourbi *et al.*, 2006). Collectively, this suggests that *o,p′*-DDT was metabolized to *o,p′*-DDD and subsequently stored in peripheral fat stores, as reported for *p,p′*-DDT metabolism (Tebourbi *et al.*, 2006). Cyp2b and Cyp3a induction may also contribute to sterol metabolism (Tabb and Blumberg, 2006) and alter circulating steroid hormone levels (Gupta *et al.*, 1980), although a poor correlation between hepatic enzyme induction and enhanced hormone clearance has been reported (You, 2004).

The induction of *Cyp2b2* and *Cyp3a23/3a1* mRNA and the differential expression of electron transport and reductive reaction–related genes such as *Ephx1*, *Gclm*, *Gpx2*, *Txn1*, and *Txnrd1* are also suggestive of an oxidative stress response. *Hmox1*, *HSPs*, and *poly (ADP-ribose) polymerases* are elevated in response to oxidative stress (Bauer and Bauer, 2002; Diller, 2006; Gero and Szabo, 2006) and were induced by *o,p′*-DDT. Reported increases in hepatic lipid peroxide content (Harada *et al.*, 2003) confirm the significance of these gene expression changes.

CAR activation is associated with cell cycle regulation (Ledda-Columbano *et al.*, 2000) and transient hepatomegaly from the induction of DNA replication and the suppression of apoptosis in response to xenobiotic exposure (Huang *et al.*, 2005). The cell proliferation–related genes, *Ccnb1*, *Ccnb2*, *Ccnd1*, *Stmn1*, and *Mdm2_predicted* (Fung and Poon, 2005; Rubin and Atweh, 2004; Tashiro *et al.*, 2007), exhibited increased expression 12–24 h after *o,p′*-DDT treatment. The induction of *Ccnd1* by the potent CAR activator TCPOBOP is abolished in *CAR* null mice (Columbano *et al.*, 2005). *Mdm2*, which activates cell cycle progression and blocks apoptosis, is also regulated by CAR (Huang *et al.*, 2005). The induction of cell proliferation–related genes suggests a transient stimulation of hepatocellular proliferation due to CAR activation, consistent with hepatocyte swelling and associated hypertrophy, and the clearance of hepatic *o,p′*-DDT and *o,p′*-DDD. Considering that short-term treatments of high-dose *p,p′*-DDT (500 ppm via diet) or repeated treatments of lower dose *p,p′*-DDT (50 or 160 ppm via diet) were required to induce cellular proliferation in the rat liver (Harada *et al.*, 2003), our data suggest that *o,p′*-DDT may also induce hepatocellular proliferation at higher doses or following repeated treatments.

Functional annotation using GO terms suggests preparation for protein synthesis by the expression of ribosomal protein

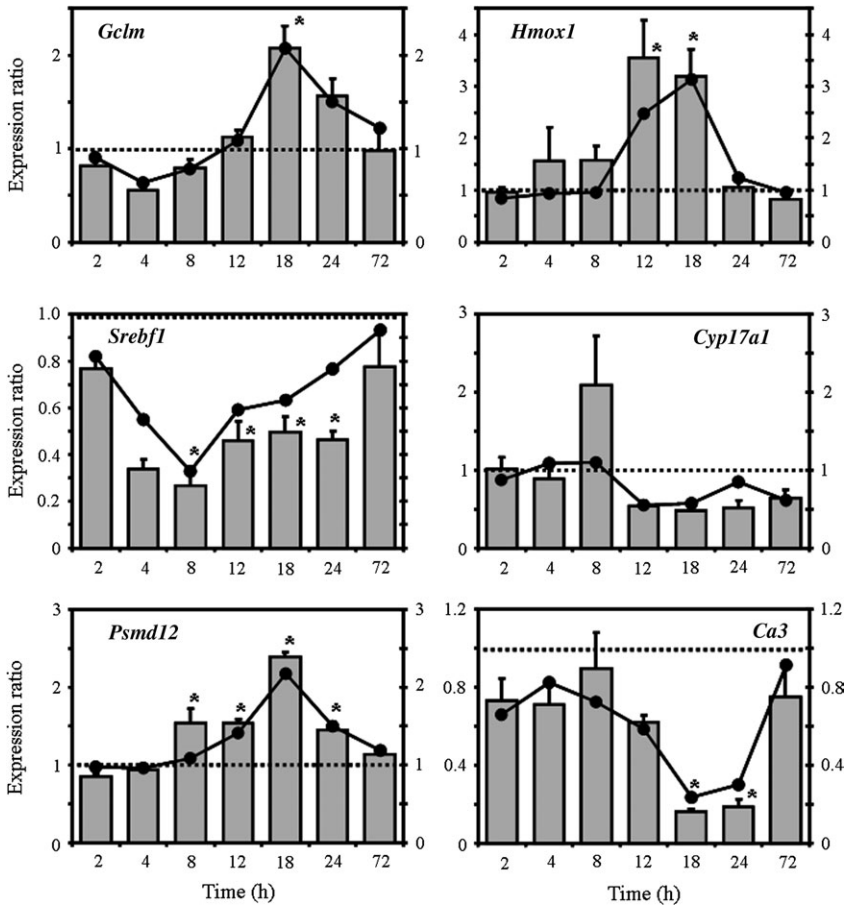

FIG. 6. QRT-PCR verification of selected microarray results. QRT-PCR results relative to time-matched vehicle controls are shown as bars (left axis) and presented as mean ± SE. Microarray results are represented as lines (right axis). The dashed line indicates the expression level of the time-matched vehicle control. The asterisk (*) indicates a significant ($p < 0.05$) difference from the time-matched vehicle controls using a two-way ANOVA followed by Tukey's post hoc test for QRT-PCR data.

genes at 18 h. The concomitant induction of proteasomal proteolysis genes would facilitate protein turnover and cellular adaptation. Both responses are consistent with the hepatocyte swelling with hypertrophy and the induction of genes associated with oxidative stress. However, the present study primarily focused on differential gene expression. Additional biochemical investigations such as protein-level analysis, enzymatic activity, or metabolite analysis are needed to demonstrate that these gene expression effects elicited by *o,p'*-DDT correlate with subsequent events.

Binding to the ER has been proposed to contribute to the hepatocarcinogenicity of *o,p'*-DDT (Giannitrapani *et al.*, 2006; Holsapple *et al.*, 2006). However, a comprehensive comparison of the hepatic differential gene expression profiles of *o,p'*-DDT–treated rat liver and EE-treated mouse liver (Boverhof *et al.*, 2004) using similar study designs and analysis methods failed to identify a correlation (Fig. 7). This analysis suggests that the hepatic gene expression effects of *o,p'*-DDT are independent of the ER, despite its estrogenicity in other tissues and models.

The activation of CAR by *o,p'*-DDT, followed by the induction of transcripts associated with oxidative stress, cell proliferation, and protein turnover, are suggestive of potential roles in the etiology of hepatocarcinogenicity (Yamamoto *et al.*, 2004). However, the carcinogenic modes of action through CAR are significantly different between rodents and humans (Holsapple *et al.*, 2006). Moreover, *o,p'*-DDT and its metabolites do not elicit agonist effects mediated by human CAR (Kretschmer and Baldwin, 2005). Consequently, the extrapolation of potential nongenotoxic carcinogenicity of DDT mediated by CAR in rodents to humans is questionable.

Furthermore, basal PXR expression is age and sex dependent and is paralleled by *Cyp3a* mRNA levels in mouse liver (Down *et al.*, 2007). The induction of *Cyp3a* genes by dexamethazone treatment also shows age and sex dependency (Anakk *et al.*, 2003; Down *et al.*, 2007). Consequently, PXR/CAR activation by *o,p'*-DDT may be affected by age and sex, which further confounds extrapolations to humans.

In summary, the differential gene expression elicited by *o,p'*-DDT in the rat liver is consistent with PXR/CAR

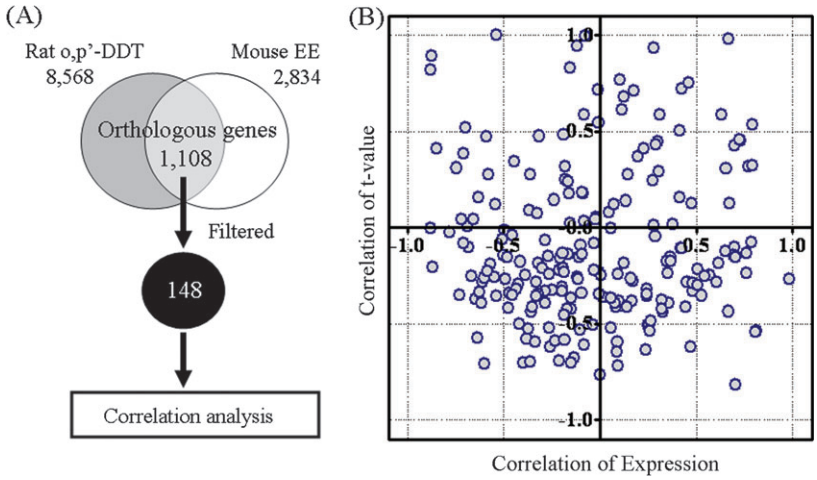

FIG. 7. Correlation analysis of *o,p′*-DDT and EE hepatic gene expression profiles. (A) Flow chart of correlation analysis. The temporal profiles of *o,p′*-DDT–treated rat liver (current study) and those of the EE-treated mouse liver (Boverhof *et al*., 2004) were compared by examining the Pearson′s correlation of the temporal gene expression (fold change) and significance ($p1[t]$ value for rat and *t*-value for mouse data) values for the 148 orthologous genes. The filtering criteria for *o,p′*-DDT study were less stringent ($p1[t]$ value > 0.99 at least at one time point and absolute fold change ≥1.5) compared to that used in GO analysis ($p1[t]$ value > 0.999 at least at two time points and absolute fold change ≥1.5). Both studies used comparable designs, models, cDNA microarray platforms, and data analysis methods. Ideally, correlations for gene expression and significance approaching 1.00 would indicate that the orthologous genes are similar and would fall in the upper right quadrant. (B) Correlation analysis. Expression and significance correlations for the 148 orthologous genes are randomly distributed throughout the plot, indicating that *o,p′*-DDT and EE gene expression profiles are poorly correlated, indicating different mechanisms of action.

regulation, and the nongenotoxic carcinogenic properties of DDT appears to be independent of the ER. Given the species differences in CAR-mediated activity, further investigation is warranted in order to more comprehensively assess the acute toxicity and probable carcinogenicity of DDT in humans.

SUPPLEMENTARY DATA

Supplementary Tables 1–3 are available online at http://toxsci.oxfordjournals.org/.

FUNDING

National Institute of General Medical Sciences (GM075838); U.S. Environmental Protection Agency (RD83184701). T.R.Z. is partially supported by the Michigan Agricultural Experiment Station.

ACKNOWLEDGMENTS

The authors would like to acknowledge Edward Dere for critical reading of the manuscript.

REFERENCES

Agrawal, A. K., and Shapiro, B. H. (2003). Constitutive and inducible hepatic cytochrome P450 isoforms in senescent male and female rats and response to low-dose phenobarbital. *Drug Metab. Dispos.* **31,** 612–619.

Anakk, S., Ku, C. Y., Vore, M., and Strobel, H. W. (2003). Insights into gender bias: Rat cytochrome P450 3A9. *J. Pharmacol. Exp. Ther.* **305,** 703–709.

Attaran, A., and Maharaj, R. (2000). Ethical debate: Doctoring malaria, badly: The global campaign to ban DDT. *BMJ* **321,** 1403–1405.

Bauer, M., and Bauer, I. (2002). Heme oxygenase-1: Redox regulation and role in the hepatic response to oxidative stress. *Antioxid. Redox Signal* **4,** 749–758.

Bayen, S., Giusti, P., Lee, H. K., Barlow, P. J., and Obard, J. P. (2005). Bioaccumulation of DDT pesticide in cultured Asian seabass following dietary exposure. *J. Toxicol. Environ. Health Part A* **68,** 51–65.

Boverhof, D. R., Fertuck, K. C., Burgoon, L. D., Eckel, J. E., Gennings, C., and Zacharewski, T. R. (2004). Temporal- and dose-dependent hepatic gene expression changes in immature ovariectomized mice following exposure to ethynyl estradiol. *Carcinogenesis* **25,** 1277–1291.

Boverhof, D. R., Kwekel, J. C., Humes, D. G., Burgoon, L. D., and Zacharewski, T. R. (2006). Dioxin induces an estrogen-like, estrogen receptor-dependent gene expression response in the murine uterus. *Mol. Pharmacol.* **69,** 1599–1606.

Burgoon, L. D., Boutros, P. C., Dere, E., and Zacharewski, T. R. (2006). dbZach: A MIAME-compliant toxicogenomic supportive relational database. *Toxicol. Sci.* **90,** 558–568.

Burgoon, L. D., Eckel-Passow, J. E., Gennings, C., Boverhof, D. R., Burt, J. W., Fong, C. J., and Zacharewski, T. R. (2005). Protocols for the assurance of microarray data quality and process control. *Nucleic. Acids Res.* **33,** e172.

Burgoon, L. D., and Zacharewski, T. R. (2007). dbZach toxicogenomic information management system. *Pharmacogenomics* **8,** 287–291.

Ciana, P., Raviscioni, M., Mussi, P., Vegeto, E., Que, I., Parker, M. G., Lowik, C., and Maggi, A. (2003). In vivo imaging of transcriptionally active estrogen receptors. *Nat. Med.* **9,** 82–86.

Cocco, P., Fadda, D., Billai, B., D'Atri, M., Melis, M., and Blair, A. (2005). Cancer mortality among men occupationally exposed to dichlorodiphenyltrichloroethane. *Cancer Res.* **65,** 9588–9594.

Columbano, A., Ledda-Columbano, G. M., Pibiri, M., Cossu, C., Menegazzi, M., Moore, D. D., Huang, W., Tian, J., and Locker, J. (2005). Gadd45beta is induced through a CAR-dependent, TNF-independent pathway in murine liver hyperplasia. *Hepatology* **42,** 1118–1126.

Dennis, G., Jr, Sherman, B. T., Hosack, D. A., Yang, J., Gao, W., Lane, H. C., and Lempicki, R. A. (2003). DAVID: Database for Annotation, Visualization, and Integrated Discovery. *Genome Biol.* **4,** P3.

Diller, K. R. (2006). Stress protein expression kinetics. *Annu. Rev. Biomed. Eng.* **8,** 403–424.

Down, M. J., Arkle, S., and Mills, J. J. (2007). Regulation and induction of CYP3A11, CYP3A13 and CYP3A25 in C57BL/6J mouse liver. *Arch. Biochem. Biophys.* **457,** 105–110.

Eckel, J. E., Gennings, C., Chinchilli, V. M., Burgoon, L. D., and Zacharewski, T. R. (2004). Empirical bayes gene screening tool for time-course or dose-response microarray data. *J. Biopharm. Stat.* **14,** 647–670.

Eckel, J. E., Gennings, C., Therneau, T. M., Burgoon, L. D., Boverhof, D. R., and Zacharewski, T. R. (2005). Normalization of two-channel microarray experiments: A semiparametric approach. *Bioinformatics* **21,** 1078–1083.

Fung, T. K., and Poon, R. Y. (2005). A roller coaster ride with the mitotic cyclins. *Semin. Cell Dev. Biol.* **16,** 335–342.

Ganem, L. G., Trottier, E., Anderson, A., and Jefcoate, C. R. (1999). Phenobarbital induction of CYP2B1/2 in primary hepatocytes: Endocrine regulation and evidence for a single pathway for multiple inducers. *Toxicol. Appl. Pharmacol.* **155,** 32–42.

Gero, D., and Szabo, C. (2006). Role of the peroxynitrite-poly (ADP-ribose) polymerase pathway in the pathogenesis of liver injury. *Curr. Pharm. Des.* **12,** 2903–2910.

Giannitrapani, L., Soresi, M., La Spada, E., Cervello, M., D'Alessandro, N., and Montalto, G. (2006). Sex hormones and risk of liver tumor. *Ann. N Y Acad. Sci.* **1089,** 228–236.

Gupta, C., Shapiro, B. H., and Yaffe, S. J. (1980). Reproductive dysfunction in male rats following prenatal exposure to phenobarbital. *Pediatr. Pharmacol. (New York)* **1,** 55–62.

Guzelian, J., Barwick, J. L., Hunter, L., Phang, T. L., Quattrochi, L. C., and Guzelian, P. S. (2006). Identification of genes controlled by the pregnane X receptor by microarray analysis of mRNAs from pregnenolone 16alpha-carbonitrile-treated rats. *Toxicol. Sci.* **94,** 379–387.

Harada, T., Yamaguchi, S., Ohtsuka, R., Takeda, M., Fujisawa, H., Yoshida, T., Enomoto, A., Chiba, Y., Fukumori, J., Kojima, S., *et al.* (2003). Mechanisms of promotion and progression of preneoplastic lesions in hepatocarcinogenesis by DDT in F344 rats. *Toxicol. Pathol.* **31,** 87–98.

Hoekstra, P. F., Burnison, B. K., Neheli, T., and Muir, D. C. (2001). Enantiomer-specific activity of o,p'-DDT with the human estrogen receptor. *Toxicol. Lett.* **125,** 75–81.

Holsapple, M. P., Pitot, H. C., Cohen, S. M., Boobis, A. R., Klaunig, J. E., Pastoor, T., Dellarco, V. L., and Dragan, Y. P. (2006). Mode of action in relevance of rodent liver tumors to human cancer risk. *Toxicol. Sci.* **89,** 51–56.

Huang, W., Zhang, J., Washington, M., Liu, J., Parant, J. M., Lozano, G., and Moore, D. D. (2005). Xenobiotic stress induces hepatomegaly and liver tumors via the nuclear receptor constitutive androstane receptor. *Mol. Endocrinol.* **19,** 1646–1653.

International Agency for Research on Cancer (IARC). (1991). *Summaries & evaluations, DDT and associated compounds,* accessed on September 26, 2007. Available at: http://www.inchem.org/documents/iarc/vol53/04-ddt.html. Accessed September 26, 2007.

Ito, N., Tsuda, H., Hasegawa, R., and Imaida, K. (1983). Comparison of the promoting effects of various agents in induction of preneoplastic lesions in rat liver. *Environ. Health Perspect.* **50,** 131–138.

Kato, N., Shibutani, M., Takagi, H., Uneyama, C., Lee, K. Y., Takigami, S., Mashima, K., and Hirose, M. (2004). Gene expression profile in the livers of rats orally administered ethinylestradiol for 28 days using a microarray technique. *Toxicology* **200,** 179–192.

King-Jones, K., Horner, M. A., Lam, G., and Thummel, C. S. (2006). The DHR96 nuclear receptor regulates xenobiotic responses in Drosophila. *Cell Metab.* **4,** 37–48.

Kitamura, S., Shimizu, Y., Shiraga, Y., Yoshida, M., Sugihara, K., and Ohta, S. (2002). Reductive metabolism of p,p'-DDT and o,p'-DDT by rat liver cytochrome P450. *Drug Metab. Dispos.* **30,** 113–118.

Kretschmer, X. C., and Baldwin, W. S. (2005). CAR and PXR: Xenosensors of endocrine disrupters? *Chem. Biol. Interact.* **155,** 111–128.

Ledda-Columbano, G. M., Pibiri, M., Loi, R., Perra, A., Shinozuka, H., and Columbano, A. (2000). Early increase in cyclin-D1 expression and accelerated entry of mouse hepatocytes into S phase after administration of the mitogen 1, 4-Bis[2-(3,5-Dichloropyridyloxy)] benzene. *Am. J. Pathol.* **156,** 91–97.

Longnecker, M. P. (2005). Invited Commentary: Why DDT matters now. *Am. J. Epidemiol.* **162,** 726–728.

Mansour, S. A. (2004). Pesticide exposure–Egyptian scene. *Toxicology* **198,** 91–115.

Martignoni, M., de Kanter, R., Grossi, P., Mahnke, A., Saturno, G., and Monshouwer, M. (2004). An in vivo and in vitro comparison of CYP induction in rat liver and intestine using slices and quantitative RT-PCR. *Chem. Biol. Interact.* **151,** 1–11.

McGlynn, K. A., Abnet, C. C., Zhang, M., Sun, X. D., Fan, J. H., O'Brien, T. R., Wei, W. Q., Ortiz-Conde, B. A., Dawsey, S. M., Weber, J. P., *et al.* (2006). Serum concentrations of 1,1,1-trichloro-2,2-bis(p-chlorophenyl)ethane (DDT) and 1,1-dichloro-2,2-bis(p-chlorophenyl)-ethylene (DDE) and risk of primary liver cancer. *J. Natl. Cancer Inst.* **98,** 1005–1010.

Meredith, C., Scott, M. P., Renwick, A. B., Price, R. J., and Lake, B. G. (2003). Studies on the induction of rat hepatic CYP1A, CYP2B, CYP3A and CYP4A subfamily form mRNAs in vivo and in vitro using precision-cut rat liver slices. *Xenobiotica* **33,** 511–527.

Minh, T. B., Kunisue, T., Yen, N. T., Watanabe, M., Tanabe, S., Hue, N. D., and Qui, V. (2002). Persistent organochlorine residues and their bioaccumulation profiles in resident and migratory birds from North Vietnam. *Environ. Toxicol. Chem.* **21,** 2108–2118.

Pedra, J. H., McIntyre, L. M., Scharf, M. E., and Pittendrigh, B. R. (2004). Genome-wide transcription profile of field- and laboratory-selected dichlorodiphenyltrichloroethane (DDT)-resistant Drosophila. *Proc. Natl. Acad. Sci. USA* **101,** 7034–7039.

Rozen, S., and Skaletsky, H. (2000). Primer3 on the WWW for general users and for biologist programmers. *Methods Mol. Biol.* **132,** 365–386.

Rubin, C. I., and Atweh, G. F. (2004). The role of stathmin in the regulation of the cell cycle. *J. Cell. Biochem.* **93,** 242–250.

Sparfel, L., Payen, L., Gilot, D., Sidaway, J., Morel, F., Guillouzo, A., and Fardel, O. (2003). Pregnane X receptor-dependent and -independent effects of 2-acetylaminofluorene on cytochrome P450 3A23 expression and liver cell proliferation. *Biochem. Biophys. Res. Commun.* **300,** 278–284.

Tabb, M. M., and Blumberg, B. (2006). New modes of action for endocrine-disrupting chemicals. *Mol. Endocrinol.* **20,** 475–482.

Tashiro, E., Tsuchiya, A., and Imoto, M. (2007). Functions of cyclin D1 as an oncogene and regulation of cyclin D1 expression. *Cancer Sci.* **98,** 629–635.

Tebourbi, O., Driss, M. R., Sakly, M., and Rhouma, K. B. (2006). Metabolism of DDT in different tissues of young rats. *J. Environ. Sci. Health B* **41,** 167–176.

Tomiyama, N., Watanabe, M., Takeda, M., Harada, T., and Kobayashi, H. (2003). A comparative study on the reliablility of toxicokinetic parameters for predicting hepatotoxicity of DDT in rats receiving a single or repeated administration. *J. Toxicol. Sci.* **28,** 403–413.

Turusov, V., Rakitsky, V., and Tomatis, L. (2002). Dichlorodiphenyltrichloroethane (DDT): Ubiquity, persistence, and risks. *Environ. Health Perspect.* **110,** 125–128.

Weissmann, G. (2006). DDT is back: Let us spray!. *FASEB J.* **20,** 2427–2429.

Willoughby, L., Chung, H., Lumb, C., Robin, C., Batterham, P., and Daborn, P. J. (2006). A comparison of Drosophila melanogaster detoxification gene induction responses for six insecticides, caffeine and phenobarbital. *Insect Biochem. Mol. Biol.* **36,** 934–942.

Wyde, M. E., Bartolucci, E., Ueda, A., Zhang, H., Yan, B., Negishi, M., and You, L. (2003). The environmental pollutant 1,1-dichloro-2,2-bis (p-chlorophenyl)ethylene induces rat hepatic cytochrome P450 2B and 3A expression through the constitutive androstane receptor and pregnane X receptor. *Mol. Pharmacol.* **64,** 474–481.

Yamamoto, Y., Moore, R., Goldsworthy, T. L., Negishi, M., and Maronpot, R. R. (2004). The orphan nuclear receptor constitutive active/androstane receptor is essential for liver tumor promotion by phenobarbital in mice. *Cancer Res.* **64,** 7197–7200.

You, L. (2004). Steroid hormone biotransformation and xenobiotic induction of hepatic steroid metabolizing enzymes. *Chem. Biol. Interact.* **147,** 233–246.